SDC-92-353

SDC
SOLENOIDAL DETECTOR NOTES

γ/π^0 SEPARATION USING THE SDC SHOWER MAXIMUM DETECTOR

October 30, 1992

A. Maghakian, P. Mélèse and R. Rusack
The Rockefeller University

SDC-92-353

γ/π^0 Separation using the SDC Shower Maximum Detector

A. Maghakian, P. Melese, R. Rusack

The Rockefeller University

October 30, 1992

1. Introduction

We have investigated the efficiency of the Shower Maximum Detector (SM) for separating gammas from neutral pions and have addressed several issues relevant to the design of the SDC SM. In this study we calculated the γ to π^0 separation efficiency for transverse energies from 20 to 60 GeV, pseudo-rapidities from 0. to 2.2 and depths between 4 and 8 radiation lengths (X_0). The bound between the barrel and the plug regions at η = 1.4 and the effect of different tower sizes at η = 2.0 was also investigated. All simulations were made for two different widths of shower maximum strips : 16 strips per tower (~ 6 mm) and 8 strips per tower (~ 12 mm).

The Monte Carlo program GEANT 3.14 was used to simulate electromagnetic showers and 500 events were generated for both γ's and π^0's for each γ/π^0 result. The photon and electron cutoffs were both 1 MeV, and it was verified that the result did not change significantly, when the cutoff was lowered to 100 keV. We only addressed the problem of resolving the two γ's, produced from π^0 decays, when they are close together in the SM detector. This analysis does not include asymmetric decays, or γ conversions within the tracking material.

2. Geometry

The geometry used in the simulation is shown in fig. 1 . It contains two regions: barrel and plug. The SM detector consists of two scintillator layers with 4 mm thickness. These planes are divided

into the towers with width $\Delta\eta x\Delta\phi = 0.05x0.05$ in the barrel. The plug towers vary: $\Delta\eta x\Delta\phi = 0.05x0.05$ for $\eta = 1.4–2.0$; $\Delta\eta x\Delta\phi = 0.1x0.1$ for $\eta = 2.0–2.5$; and $\Delta\eta x\Delta\phi = 0.2x0.2$ for $\eta = 2.5–3.5$. The SM is positioned within the electromagnetic calorimeter, which consist of 4 mm thick lead and scintillator layers. The barrel region also contains three aluminum planes (~ $1X_0$ in total) before the EM calorimeter, which simulates the magnetic coil. A uniform magnetic field of 2 T inside the coil is assumed.

These studies were done for two different geometrical configu - rations of SM :

1) Constant radiation length ($6X_0$) of material before SM and therefore different depths of SM within the EM calorimeter for different angles, as shown in Fig. 1 .

2) Fixed position of SM (after 4 lead/scintillator layers of EM calorimeter) and therefore different radiation length before SM for different angles.

3. Analysis

The main idea of the analysis is as follows. We defined an "average photon profile" as the SM transverse profile (energy verses SM bin) normalizing the total energy and averaging over all photon showers by superimposing the highest SM bin. Figure 2 shows such an average photon profile for 20 GeV, $\eta = 1.3$, where the error bars represent the rms fluctuations for each bin. We fit the individual γ and π^0 events to this distribution, weighting by the rms error for each bin, and calculate the χ^2 of the fit . Figure 3 shows both a photon and π^0 events fitted to the average photon profile. As a rule, the SM profile for single gamma events are closer to the average γ profile ($\chi^2 \sim 1$ on average) than for pions, therefore the χ^2 values for π^0 are bigger.

This analysis was done separately for each η and ϕ view of the SM and then the maximum of the two χ^2 was chosen. Frequently, the two photons, produced by a π^0, look like a single photon in one of the views, but are very well separated in the other. The average χ^2 washes out some information about separation. On the other hand, single photons are more symmetric in the two views, and therefore $\max(\chi^2) \sim \bar{\chi}^2$.

For example, for E_T = 30 Gev η = 1.4

$$< \bar{\chi}^2{}_\gamma >= 1 \text{ (by def.)} \quad \text{and} \quad < \bar{\chi}^2{}_\pi > \sim 3.$$

while

$$< \max(\chi^2{}_\gamma) > \sim 1.3 \quad \text{and} \quad < \max(\chi^2{}_\pi) > \sim 35.$$

(< > means average over all events) .

In the above procedure, we actually determined the shower centroid position and divided the average γ profile into 5 profiles according to the centroid's relative position within the strip. Then the individual events were fit to the one of the 5 profiles according to it's centroid impact parameter. Figure 4 shows an example of two average profiles, one in which centroid impacts to the left of center (a), and the other to the right (b). This approach is especially successful for wide strips (8 strips per tower) and improves the π^0 rejection by 10 - 15%.

In the analysis we only analyzed π^0's, that had both photons fall within a window, defined as +/- 8 strips (assuming 8 strips per EM tower) with respect to the highest SM bin. Changing the window size from +/- 4 to +/- 12 changes the π^0 rejection by less than 5%. The analysis in this note does not address the asymmetric π^0 decays.

Finally, we have values of χ^2 corresponding to each gamma or pion event. Figure 5 shows these χ^2 distributions for E_T = 30 GeV, η = 0. Gamma acceptance and pion rejection functions are defined by varying the threshold on χ^2 as shown in figure 6 for the same case (E_T = 30 GeV, η = 0). As the χ^2 threshold increases, the γ acceptance decreases and the percentage of π^0's rejected increases. For this analysis we present the π^0 rejection for 80% photon acceptance as a single measure of performance, for instance 92% π^0 rejection from figure 6. In this case 20% pion rejection corresponds to no distinction between the χ^2 distributions of π^0's and γ's.

4. Results

The results for π^0 rejection at 80% γ acceptance vs. rapidity and transverse energy are shown on figures 7 and 8. We have found that for the barrel region, the separation is roughly the same (a little better for big η as result of geometry and our separation technic). The separation improves at higher η because the decrease in opening angle, as E_0 increases for fixed E_T, is offset by the larger distance

between the interaction point and the SM. In addition, the π^0 separation is improved at higher η because of the projection of the γ's onto the SM plane. For the plug region the separation gets worse as η increases, because the angle between photons is small for the same transverse energy, but the distance between the interaction point and SM is not increasing with the angle as for the barrel region. There is a strong energy dependence for both regions and the separation is very sensitive to the size of the strips (8 vs. 16 strips per tower).

The data in figures 7 and 8 at η = 1.4 and η = 2.0 are the average over the results for boundaries between the barrel and the plug regions and the one between different tower sizes . We investigated these boundaries separately and found that the separation at the ends of the barrel and plug regions in the point η = 1.4 is practically the same (figure 9), and it is very sensitive to the changing of tower size (0.05x0.05 to 0.1x0.1) at the point η = 2.0 (figure 10). These results are easy to explain from geometry : the strip size on the edges of the barrel and plug (η = 1.4) are the same and at η = 2.0 it changes from 8 mm to 14.5 mm. Therefore the separation doesn't change at η = 1.4, but there is a big jump at η = 2.0.

We also simulated the configuration in which the SM is positioned after different amount of material. It was found that the separation is practically the same for 4 X_0 and $6X_0$ at η = 0. (figure 9), within statistical fluctuations. It is more sensitive for high energies and wide strips, and for these cases the separation is better at 4 X_0 . The separation is worse for $8X_0$ compared to $6X_0$ at η = 1.3 (figure 10) and this difference exists for all energies and different strip sizes.

5. Conclusion

. We have studied the γ/π^0 separation for different values of η, energies, sizes of strips and amounts of tracking material.

The π^0 rejection very sensitive to the different transverse energies and sizes of strips. It improves at low energies because the

angle between the two photons from the π^0 are wider for lower energies. The narrow strips simply have better resolution.

All results for the different rapidities, including boundaries, are easy to explain qualitatively from the geometry of the simulated detector. The separation is better in the barrel region, especially for big eta's, and worse in the plug.

The separation is practically the same for 4 X_0 and $6X_0$ at $\eta = 0$, but worse for $8X_0$ compared to $6X_0$ at $\eta = 1.3$.

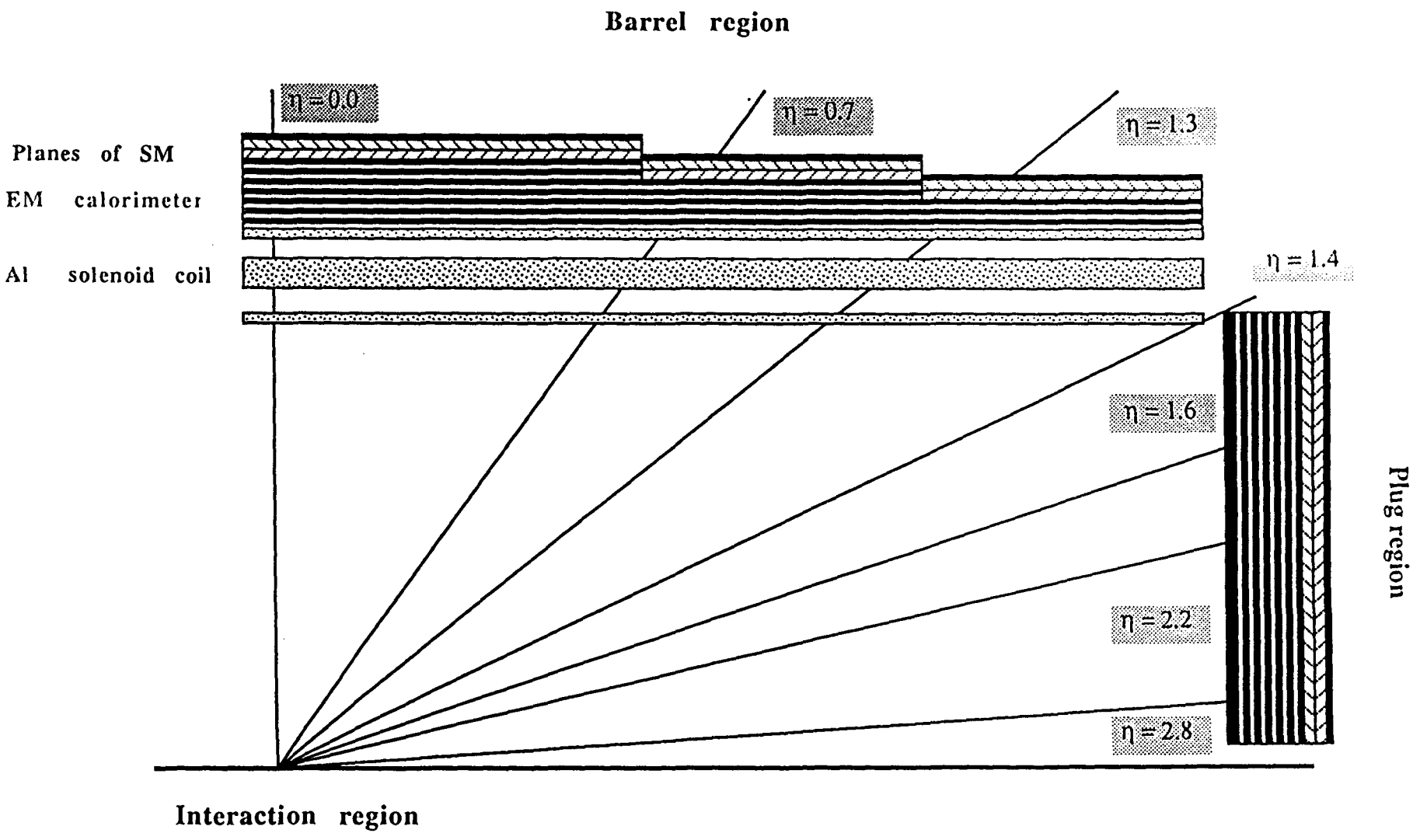

Figure 1: Geometry of the simulated SDC detector

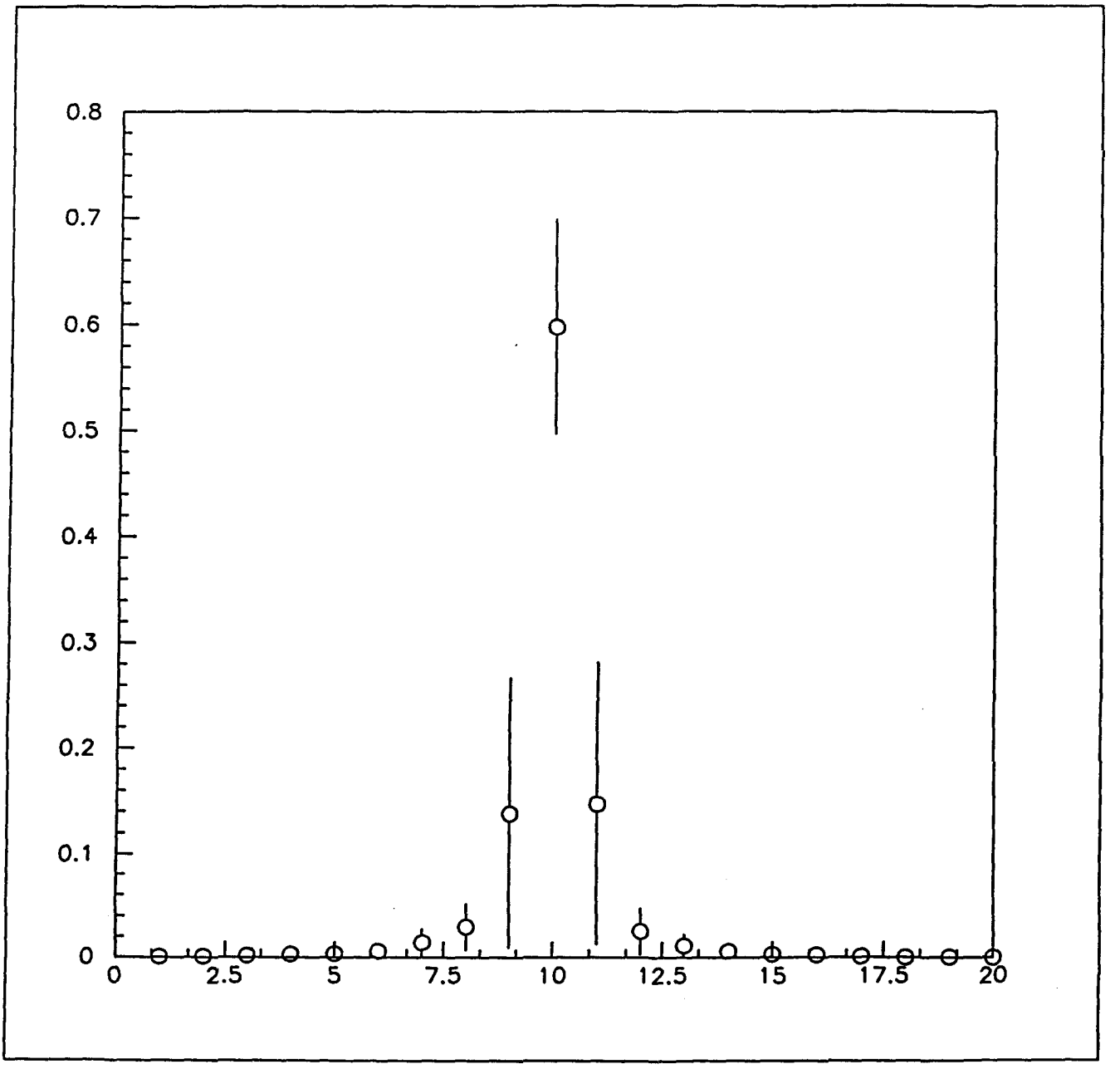

Figure 2 : Standard γ distribution for E = 20 GeV, η = 1.3

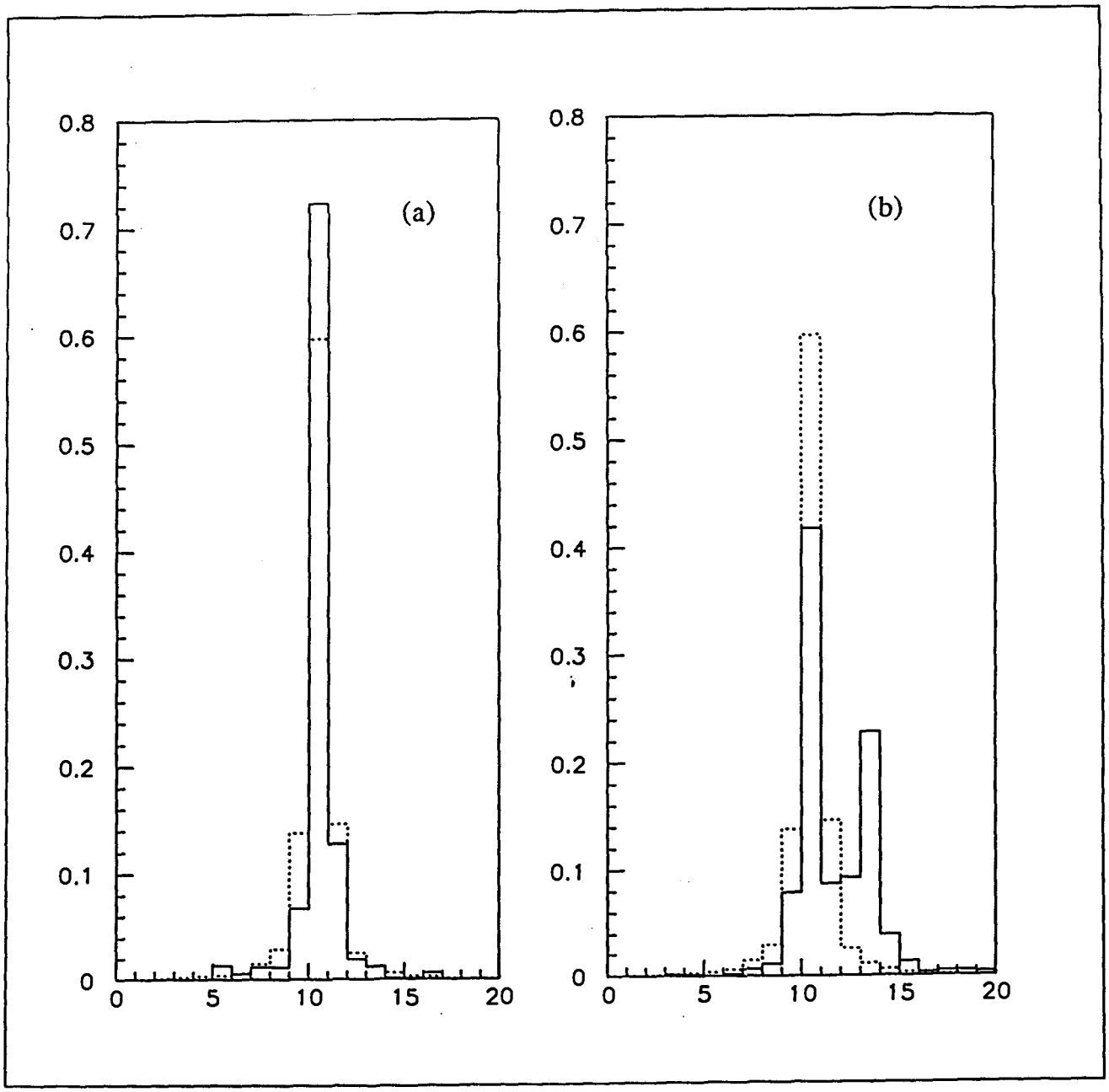

Figure 3 : γ and π^0 events fitted to the standard γ distribution.
(a) solid line - γ event, dot line - γ distribution, $\chi^2 = 0.6$
(b) solid line - π^0 event, dot line - γ distribution, $\chi^2 = 34$.

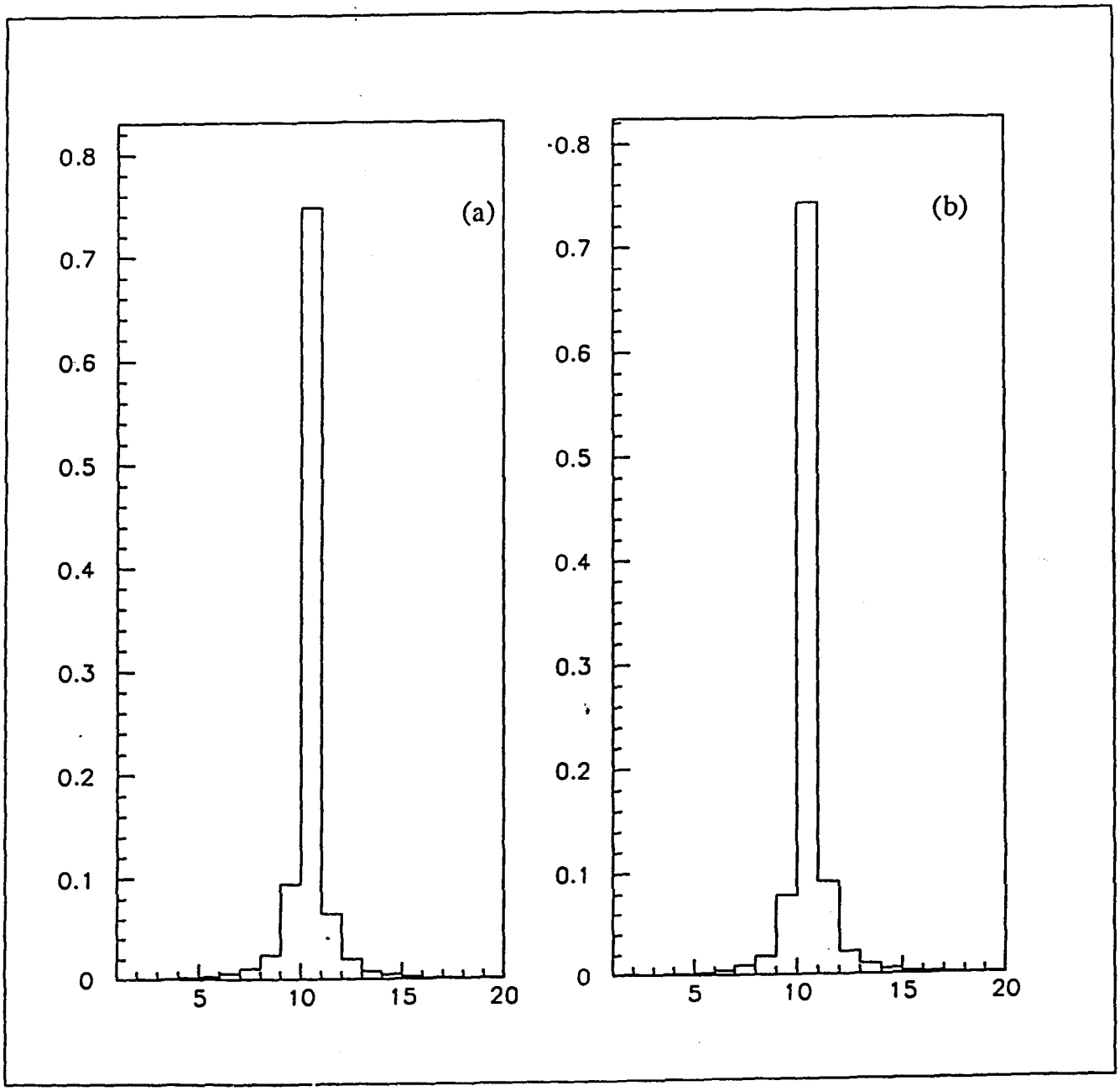

Figure 4 : Two different average γ distributions for the different positions of centroid .
(a) Centroid impacts to left of center of the strip
(b) Centroid impacts to right of center of the strip

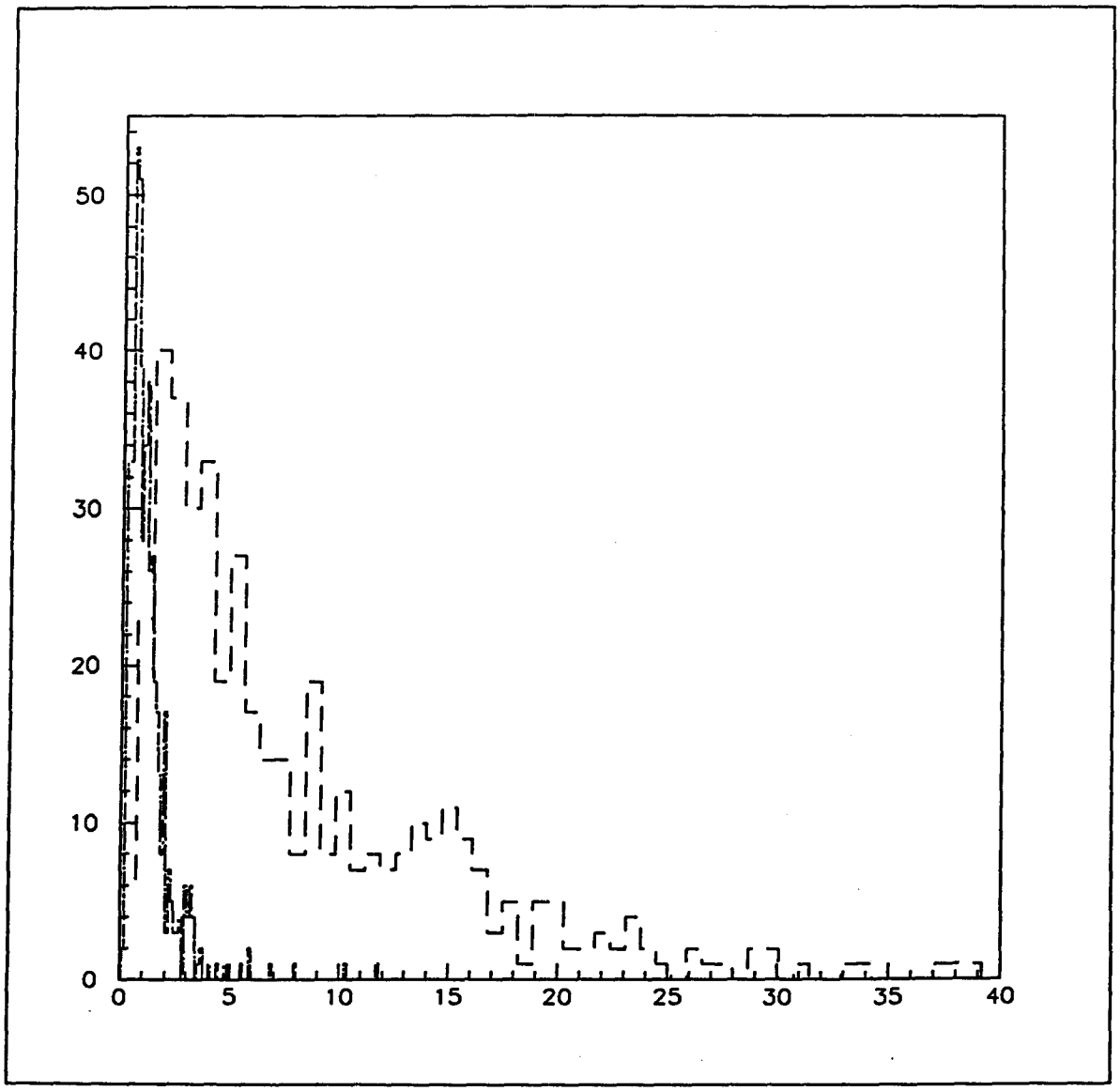

Figure 5 : γ and π^0 χ^2 distributions (γ - solid line, π^0 - dot line) for E = 30 Gev, η = 0., 16 strips per tower

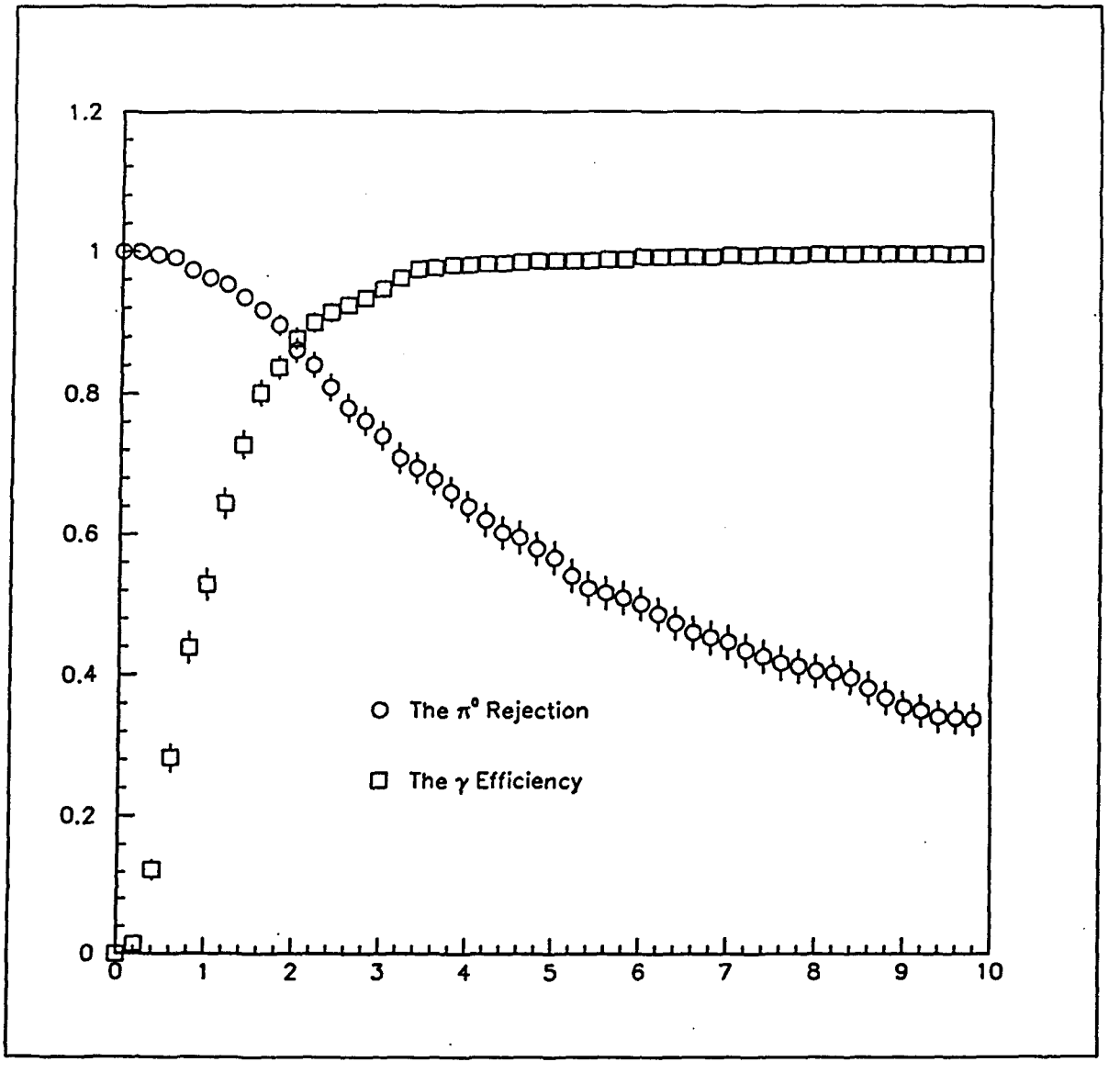

Figure 6 : π^0 rejection and γ acceptance vs χ^2 cuts
E = 30 GeV, η = 0., 16 strips per tower

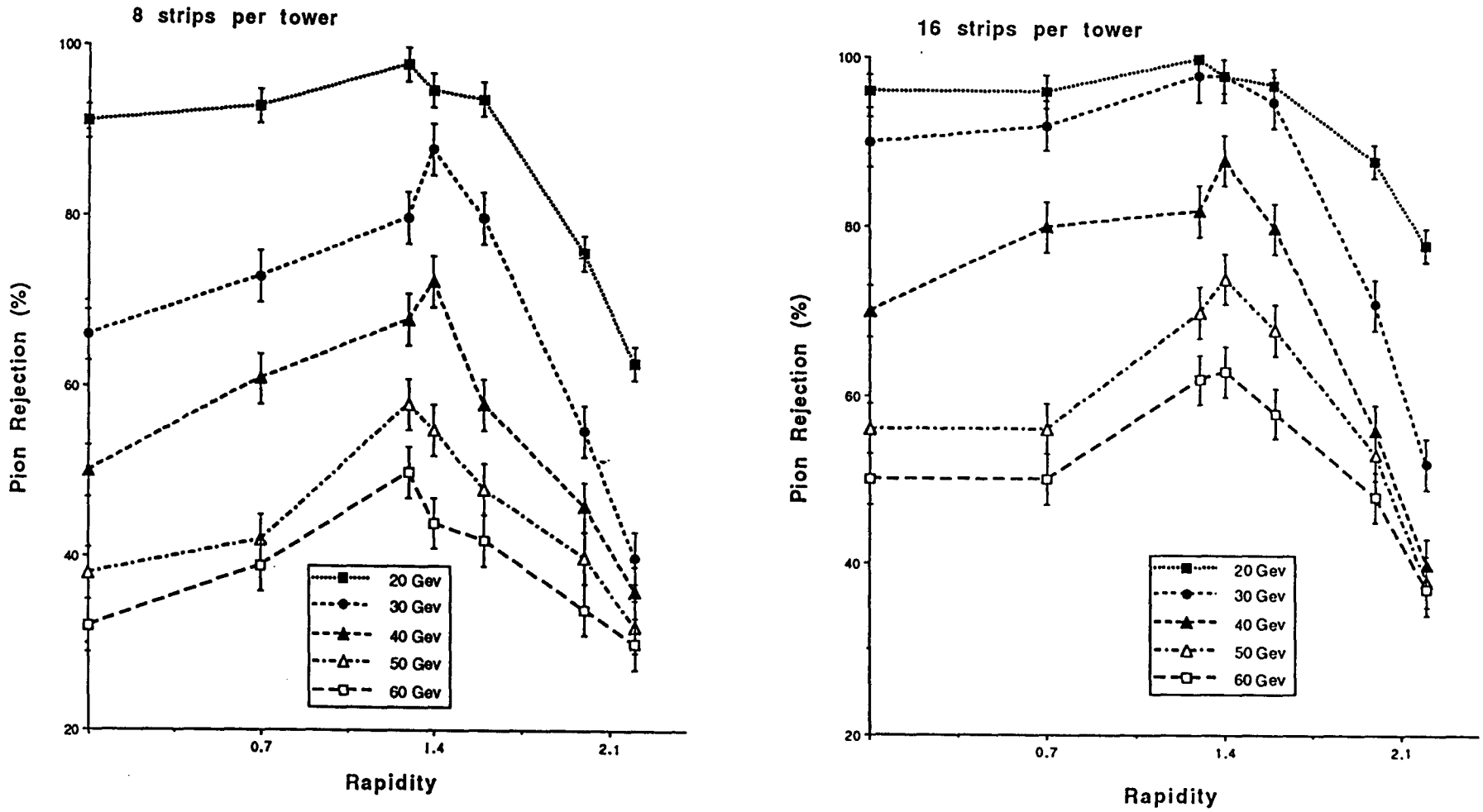

Figure 7 : Pizero rejection for 80% gamma efficiency vs. rapidity

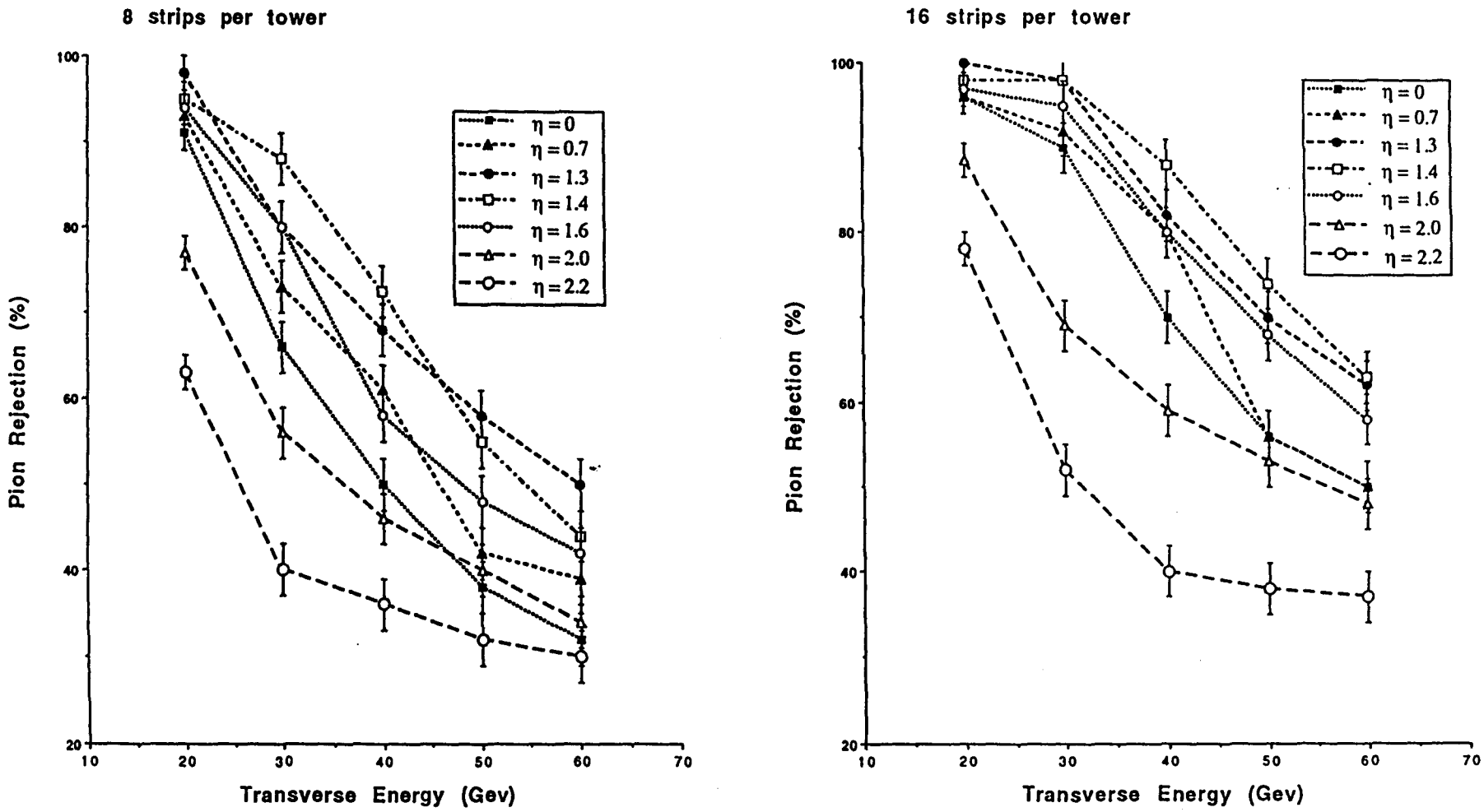

Figure 8 : Pizero rejection for 80% gamma efficiency vs. transverse energy

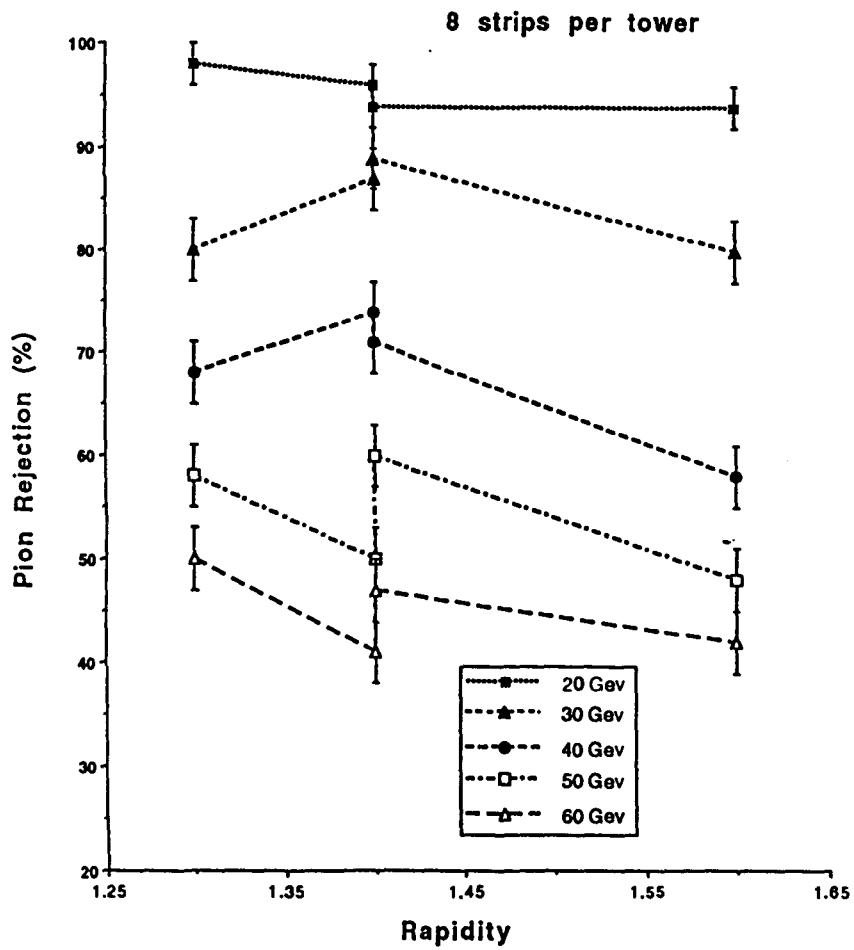

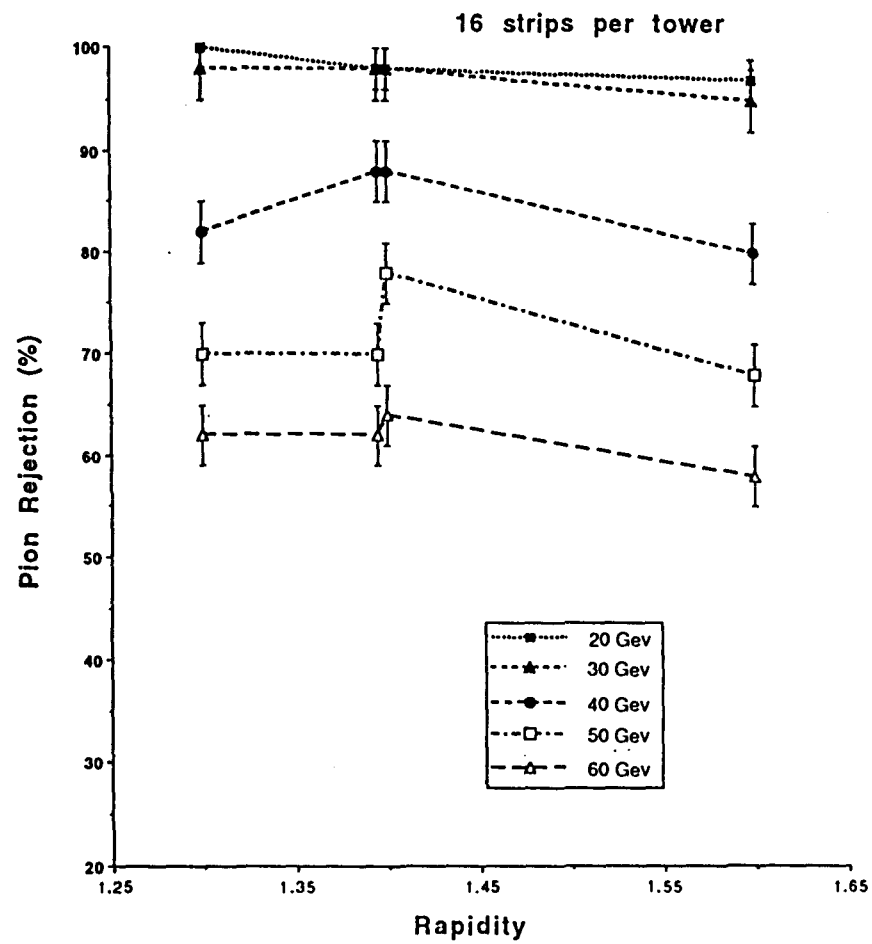

Figure 9 : Pizero efficiency for 80% gamma rejection.
Transition between barrel and plug regions in point $\eta = 1.4$

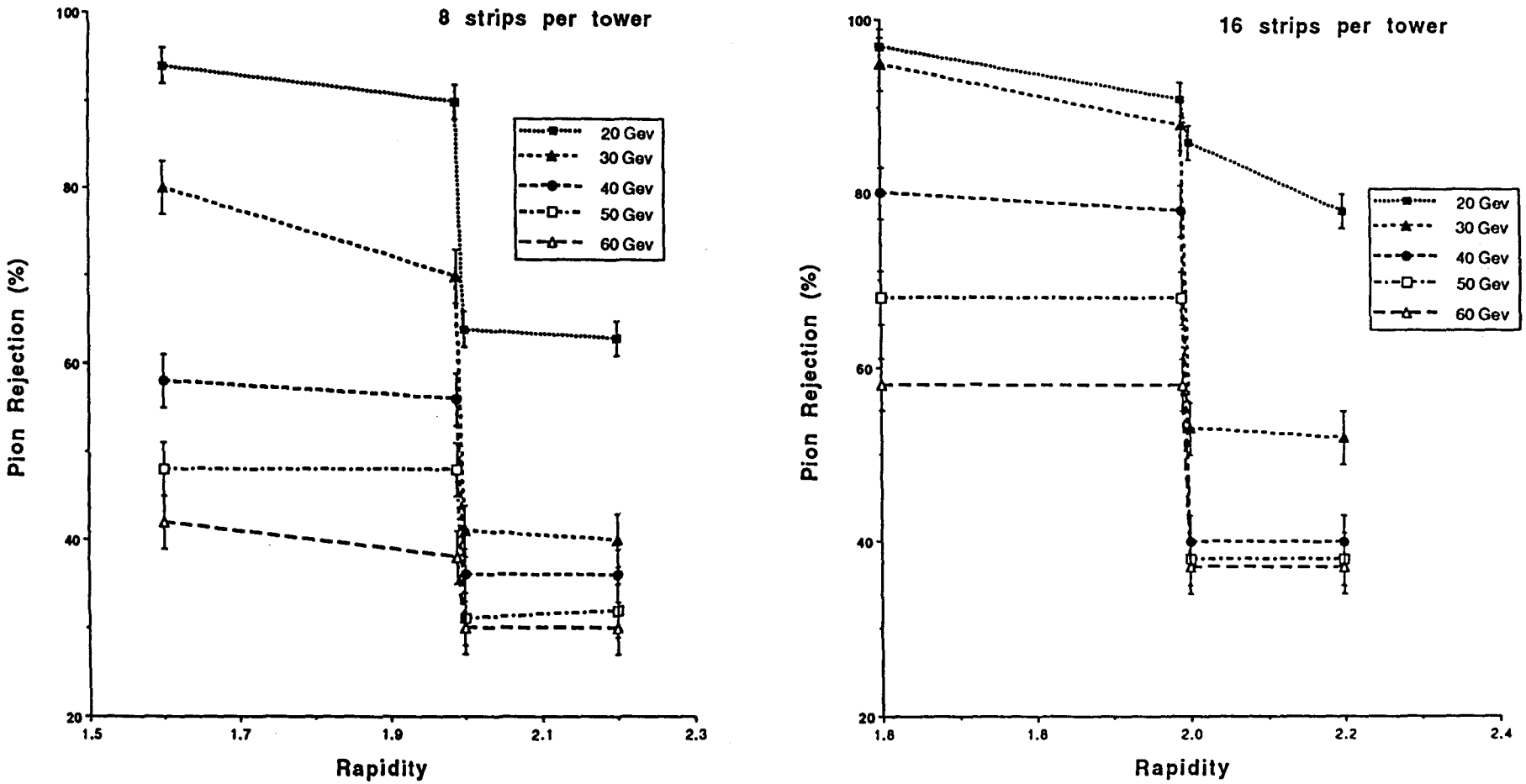

Figure 10 : Pizero rejection for 80% gamma efficiency.
Transition from tower with size (0.05,0.05) to (0.1,0.1) in point $\eta = 2.0$

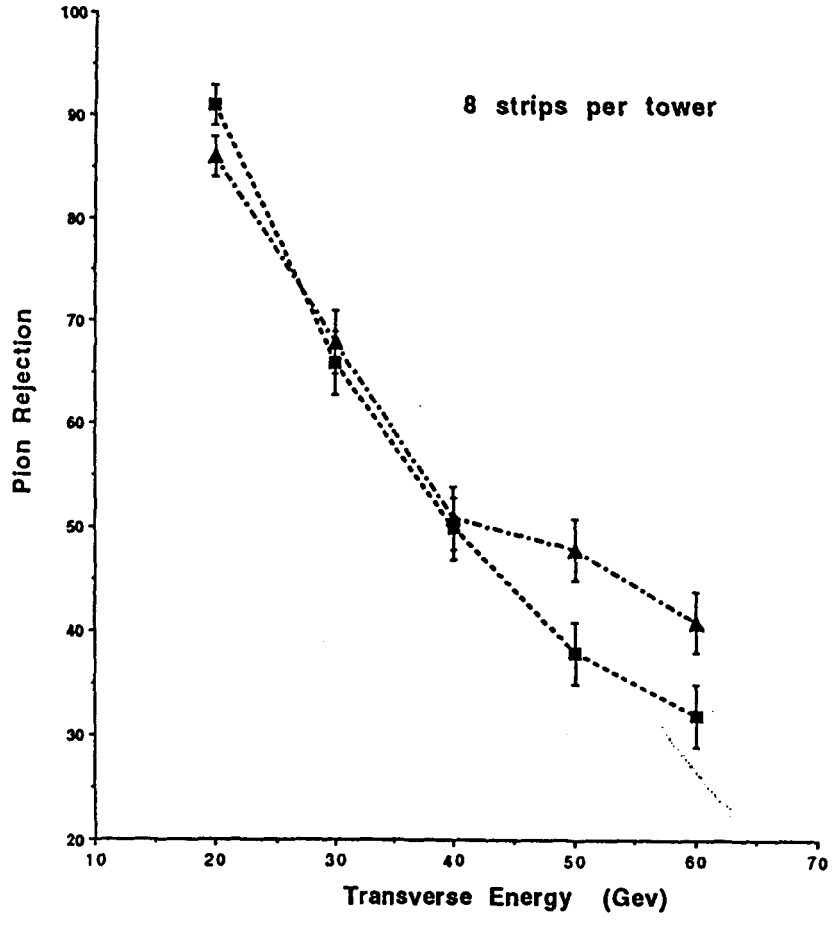

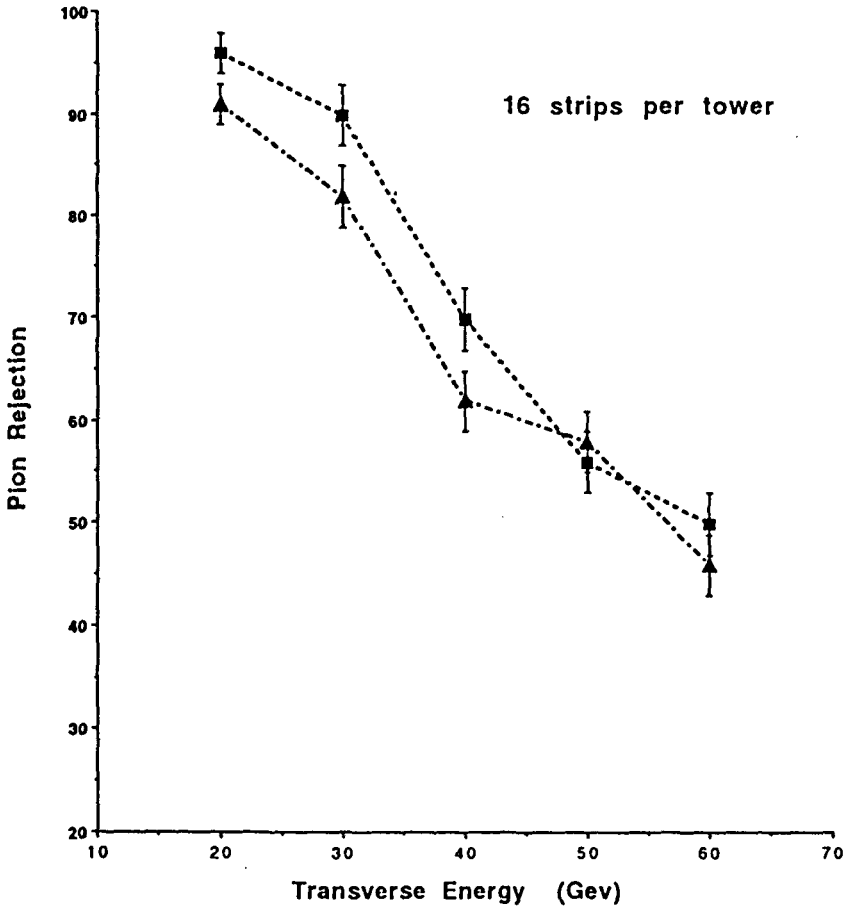

Figure 11 : Comparision of pizero rejections for 80% gamma efficiency in SM positioned after 4 (--▲--) and 6 (--■--) radiation length. $\eta = 0$

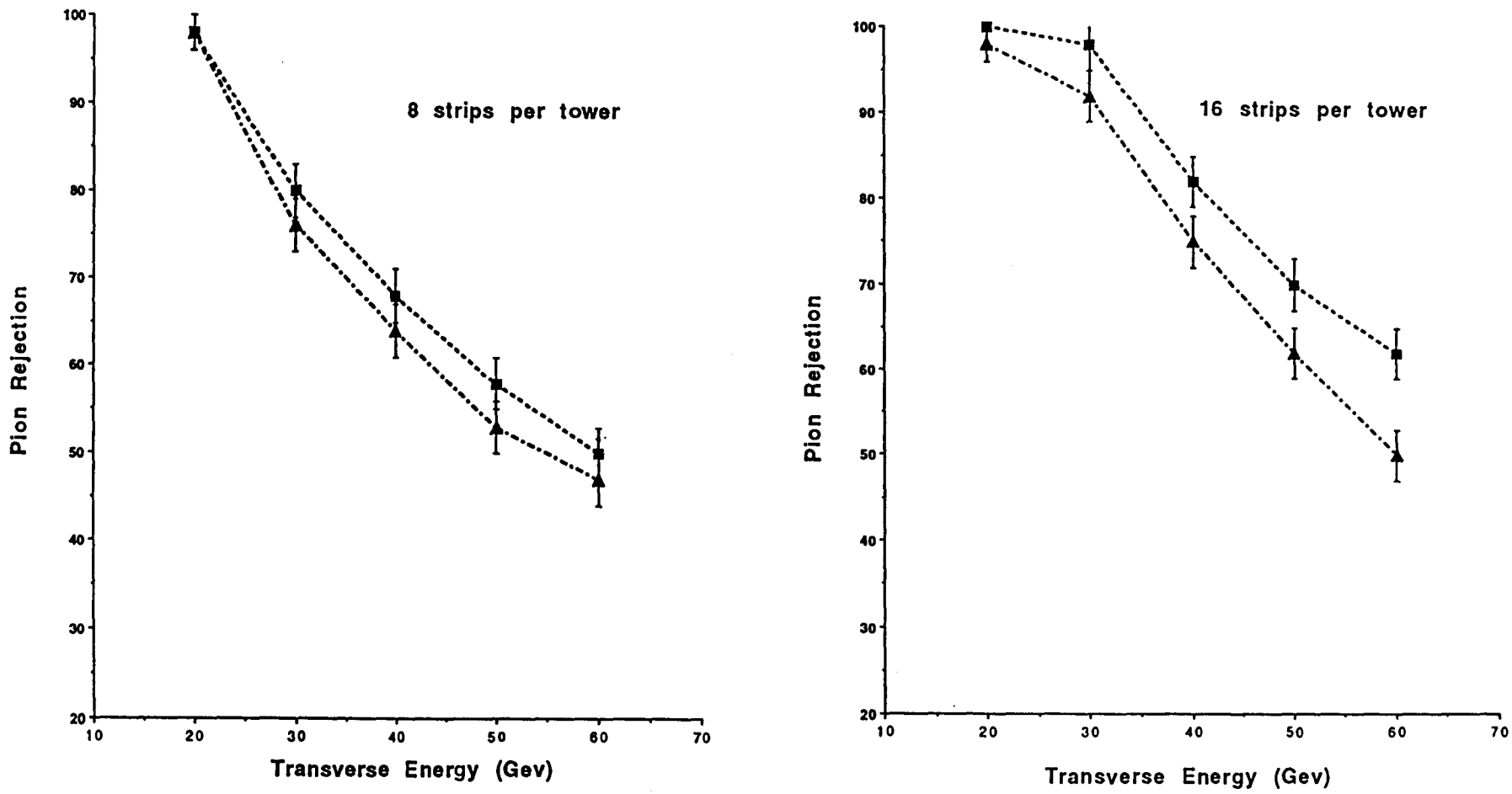

Figure 12 : Comparision of pizero rejection for 80% gamma efficiency in SM positioned after 6 (-■-) and 8 (··▲··) radiation length. $\eta = 1.3$